REPORT

CHEMICAL PHYSICS

Second critical point in two realistic models of water

Pablo G. Debenedetti[1]*†, Francesco Sciortino[2]†, Gül H. Zerze[1]†

The hypothesis that water has a second critical point at deeply supercooled conditions was formulated to provide a thermodynamically consistent interpretation of numerous experimental observations. A large body of work has been devoted to verifying or falsifying this hypothesis, but no unambiguous experimental proof has yet been found. Here, we use histogram reweighting and large-system scattering calculations to investigate computationally two molecular models of water, TIP4P/2005 and TIP4P/Ice, widely regarded to be among the most accurate classical force fields for this substance. We show that both models have a metastable liquid-liquid critical point at deeply supercooled conditions and that this critical point is consistent with the three-dimensional Ising universality class.

Water affects virtually every aspect of our lives and sculpts the physical environment that we inhabit (*1*); it is a key actor in the major physical and chemical processes that are essential to life as we know it (*2*). Water's ubiquity masks the fact that many of its physical properties are qualitatively different from those of most other substances: Liquid water at ambient pressure is denser than the solid into which it freezes; cold liquid water expands upon cooling and becomes less viscous upon compression; and water has at least 17 crystalline phases (*3*). These are just a few of the numerous examples of water's distinctiveness, which originates in its ability to form hydrogen bonds and the consequent tetrahedral coordination to which they, in conjunction with the water molecule's geometry, give rise (*4*). Tetrahedrally coordinated liquids such as silica and silicon share many of water's anomalies (*5*). The microscopic origin of these anomalies is the liquid's ability to form transient local arrangements characterized by low density, low energy, and low entropy (*6*, *7*).

In 1976, experiments by Speedy and Angell brought to light the fact that water's distinctive behavior becomes more pronounced upon supercooling (*8*). The sharp increases in liquid water's response functions (isothermal compressibility, isobaric heat capacity, and magnitude of the thermal expansion coefficient) upon cooling imply a corresponding enhancement of fluctuations (density, enthalpy, and entropy-volume covariance, respectively) (*6*, *7*). Providing an experimentally testable thermodynamically consistent explanation for these observations has since become a major goal for researchers, one that remains only partially fulfilled to date. A number of thermodynamic scenarios have been formulated that can explain experimental observations (*7*, *9*–*11*), but an unambiguous experimental discrimination among them has not yet been possible. The difficulty of performing measurements under conditions where the liquid is highly metastable with respect to the crystal, hence short-lived, remains a challenge to experimental ingenuity. Much progress has nevertheless been made in the characterization of cold, metastable forms of water in the supercooled (*12*, *13*), stretched (*14*), and glassy states (*15*).

An intriguing hypothesis was formulated in a 1992 computational study, according to which the enhanced fluctuations upon supercooling are indicative of an underlying first-order phase transition between two liquid phases, terminating at a liquid-liquid critical point (LLCP) located at higher-than-atmospheric pressure (*16*). The verification or falsification of the liquid-liquid phase transition (LLPT) hypothesis has been a major goal of experimental studies. Although no definitive proof of the existence of a metastable second critical point in water has been produced to date (*17*), the preponderance of evidence is consistent with this hypothesis (*18*, *19*).

Computational studies have played a central role in this field (*20*), because crystallization, which poses a major challenge in experiments, does not affect simulations. Indeed, in molecular models of water, the characteristic time scales for relaxation and crystal nucleation are well separated (*21*), enabling the accurate thermodynamic characterization of metastable liquid states without the interference of crystallization. These time scales are not as widely separated in atomic models of water (*22*), where avoiding crystallization at deeply supercooled conditions is a challenge.

Rigorous proof of the existence of a LLPT requires performing free energy calculations at subcritical temperatures, a computationally demanding undertaking. Although evidence consistent with a LLPT has been reported for several potentials (*20*, *23*, *24*), to date, rigorous proof of the existence of a LLPT has only been

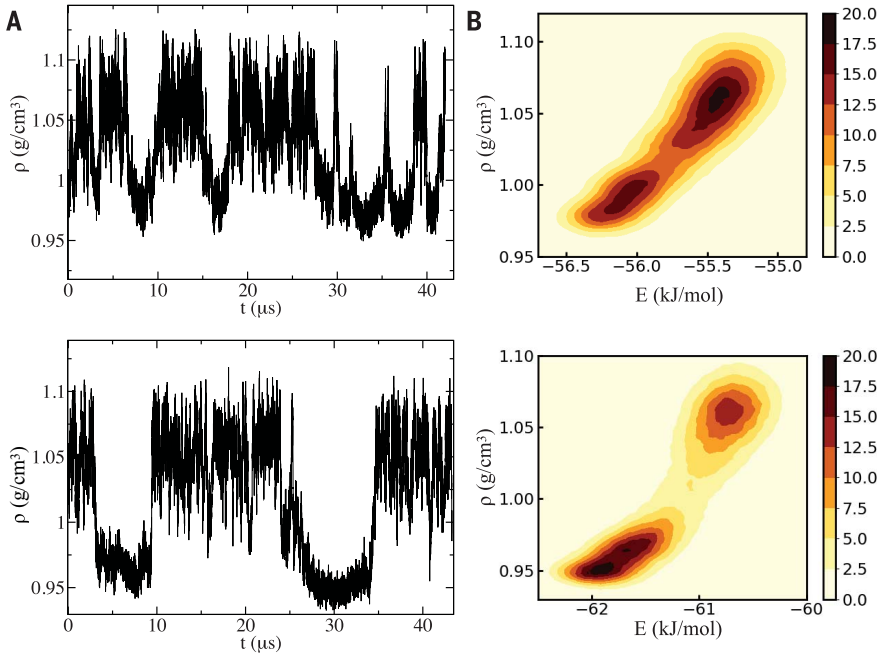

Fig. 1. Critical density and energy fluctuations. (**A**) Density fluctuations during isobaric molecular dynamics simulations in the vicinity of the critical point for N = 300 molecules of (top) TIP4P/2005 at 177 K and 1750 bar and (bottom) TIP4P/Ice at 190 K and 1725 bar. (**B**) Statistics of critical fluctuations displayed as two-dimensional (density and energy) probability densities for TIP4P/2005 (top) and TIP4P/Ice (bottom) at their respective critical points (see also Fig. 2).

[1]Department of Chemical and Biological Engineering, Princeton University, Princeton, NJ, USA. [2]Department of Physics, Sapienza University of Rome, Rome, Italy.
*Corresponding author. Email: pdebene@princeton.edu
†These authors contributed equally to this work.

obtained for the ST2 model (*25*–*28*), a five-site model in which tetrahedrality is built into its constitutive geometry.

Here, we uncover critical behavior in two water models for which a LLPT has yet to be rigorously proven. We performed histogram reweighting (*29*) and large-system scattering calculations using two of the most accurate classical models of water, TIP4P/2005 (*30*) and TIP4P/Ice (*31*). Unlike in the ST2 model, the interacting sites in both TIP4P models lie on the same plane. We applied the theory of critical phenomena and statistical mechanical analysis to quantify density and energy fluctuations close to the critical point. We obtained evidence of critical behavior belonging to the three-dimensional (3D) Ising universality class, which demonstrates that, in addition to the regular vapor-liquid critical point, both TIP4P/2005 and TIP4P/Ice exhibit a second, metastable critical point at deeply supercooled conditions.

Figure 1A shows the temporal evolution of the density for TIP4P/2005 (top) and TIP4P/Ice (bottom), obtained from extremely long (>40 μs) isobaric-isothermal molecular dynamics simulations at slightly supercritical conditions (see supplementary text section of the supplementary materials and tables S1 and S2). Pronounced density fluctuations, characteristic of near-critical behavior, are evident. The statistics of these critical fluctuations are displayed in Fig. 1B for TIP4P/2005 (top) and TIP4P/Ice (bottom), in the form of two-dimensional probability densities, reweighted to the respective critical points using the multiple histogram method (Fig. 2 and fig. S1). Bimodal behavior, as well as a strong positive correlation between density and energy fluctuations, is evident. Both models experienced strong fluctuations between low density–low energy and high density–high energy states, and these states also differ in their structural properties (fig. S2). The time scales for relaxation and crystal nucleation remained well separated across the range of conditions probed in this work (fig. S3). A nucleation event, being irreversible, would prevent the density from oscillating between low and high values. The ergodicity of the simulated systems at the conditions explored in this work is documented in figs. S4 and S5.

Figure 2, A and B, shows the statistics of density fluctuations at selected temperatures for pressure values at which the variance of density fluctuations is maximized. The distributions were obtained using the multiple histogram method. The appearance of two peaks, characteristic of critical phenomena, signals the coexistence of regions of different density, correlated over distances comparable to the studied system size.

To ascertain the universality class of the metastable critical point, we compared the

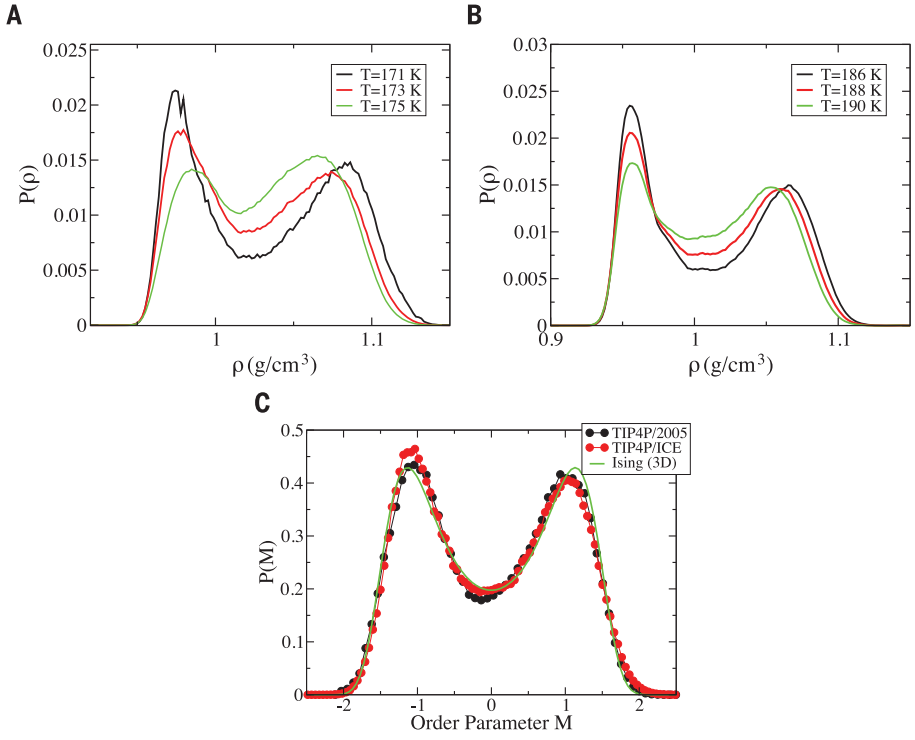

Fig. 2. Universal Ising-like behavior of order parameter fluctuations. Density probability distributions for (**A**) TIP4P/2005 and (**B**) TIP4P/Ice, obtained from density fluctuation data collected at several *T* and *P* and then reweighted to arbitrary state points using the histogram reweighting procedure (see supplementary materials). The pressure at each temperature was chosen so as to maximize the variance of the density distribution. (**C**) Simulation data (symbols) for the order parameter distribution ($M = \rho + sE$) matched to the corresponding 3D Ising universal distribution (green curve). The match yields optimal values for *s*, T_c (172 and 188.6 K for TIP4P/2005 and TIP4P/Ice, respectively), and P_c (1861 and 1725 bar for TIP4P/2005 and TIP4P/Ice, respectively) (table S3). $N = 300$ molecules.

distribution of order parameter fluctuations with the corresponding asymptotic form for the 3D Ising model. The relevant order parameter for single-component fluids is a linear combination of density and configurational energy ($\rho + sE$), where *s* is a field-mixing parameter (*32*). As described in the supplementary materials, we performed a nonlinear fit to regress the critical temperature T_c, critical pressure P_c, and field-mixing parameter such that the reweighted order parameter fluctuations best match the theoretical predictions. The quality of the fits shown in Fig. 2C for a system size of $N = 300$ water molecules (see figs. S6 and S7 for other system sizes) confirmed that the finite-size estimates of the metastable critical point for TIP4P/2005 and TIP4P/Ice are consistent with the 3D Ising universality class. Averaging over the three small-system estimates ($N = 300$, 500, and 1000 water molecules), our best estimate for the critical point is $T_c = 172 \pm 1$ K and $P_c = 1861 \pm 9$ bar for TIP4P/2005 and $T_c = 188 \pm 1$ K and $P_c = 1739 \pm 6$ bar for TIP4P/Ice (table S3).

To explore the anomalous scattering behavior expected in the vicinity of a LLCP (*33*), we computed the oxygen-oxygen static structure factor $S(k)$, focusing on the small–wave vector region (small k). The static structure factor is given by

$$S(k) = N^{-1}\sum_{j=1}^{N}\sum_{l=1}^{N}\left\langle e^{[i\mathbf{k}\cdot(\mathbf{r}_j-\mathbf{r}_l)]}\right\rangle \quad (1)$$

where the angle brackets denote thermal averaging and averaging over wave vectors $\mathbf{k}$ with the same magnitude k. The structure factor is related to the isothermal compressibility by

$$\lim_{k\to 0} S(k) = \rho k_B T K_T \quad (2)$$

In the above equations, N is the number of molecules, $\mathbf{r}_m$ is the position vector of the oxygen of molecule m, ρ is the number density, k_B is the Boltzmann constant, and K_T is the isothermal compressibility.

In the Ornstein-Zernike approximation (*34*), which is valid in the small-k limit, $S(k)$ close to a critical point can be written as

$$S(k) = S_N(k) + \frac{S_A(0)}{\xi^2 k^2 + 1} \quad (3)$$

where S_N is the normal component of the structure factor (not affected by critical fluctuations), S_A quantifies the contribution of critical (anomalous) fluctuations to the compressibility (see

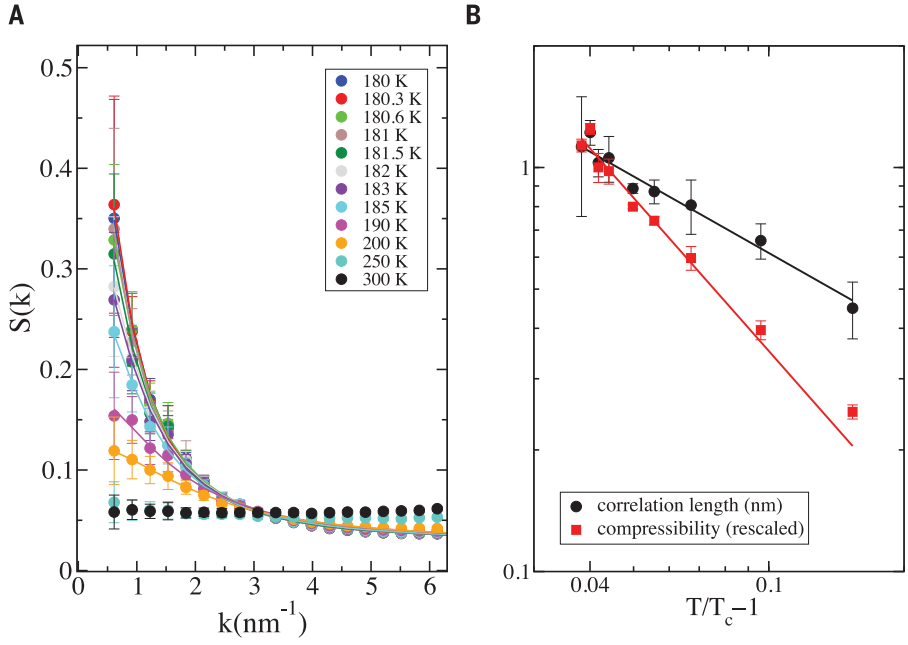

Fig. 3. Anomalous behavior of the structure factor near the critical point. (**A**) Low-*k* region of the structure factor computed for N = 36,424 TIP4P/2005 molecules at different temperatures and ρ = 1.012 g/cm^3, in proximity to the critical isochore (see supplementary materials). (**B**) Calculated values of the isothermal compressibility (Eq. 2) in units of inverse pascal, and scaled by a multiplication factor of 2 × 10^8, and the correlation length (Eq. 3). The slope of the lines through the data correspond to the 3D Ising critical exponents (ν = 0.63 and γ = 1.26; see Eqs. 4 and 5). Critical temperature obtained by a constrained least-squares fit to the data, yielding T_c = 173.3 K. Errors are standard deviations obtained using three equal, nonoverlapping data blocks.

Eq. 2), and ξ is the correlation length, i.e., the characteristic distance over which density fluctuations become uncorrelated. Thus, by computing $S(k)$ according to Eq. 1 over a range of wave vectors and fitting to Eq. 3 (fig. S8), one can obtain numerically, for a given T, the quantities $S_N(k)$, $S_A(0)$, and ξ. Asymptotically close to the critical point, the Lorentzian form in Eq. 3 should be replaced by $S(k) \sim (\xi^2 + k^2)^{\left(\frac{\eta}{2}-1\right)}$, with η ≈ 0.04 (*35*, *36*); at the temperatures sampled in this work (table S4), the proportionality between $1/S(k)$ and k^2 was satisfied (fig. S9), indicating that the Ornstein-Zernike form (Eq. 3) is valid, and η corrections were negligible.

In the vicinity of the critical point, the correlation length and the isothermal compressibility are expected to diverge along the critical isochore according to (*36*)

$$K_T \sim \left(\frac{T}{T_c} - 1\right)^{-\gamma} \quad (4)$$

$$\xi \sim \left(\frac{T}{T_c} - 1\right)^{-\nu} \quad (5)$$

For the 3D Ising universality class, the critical exponents are ν ≈ 0.63 and γ = 2ν ≈ 1.26. Figure 3A shows the computed structure factor as a function of $k = |\mathbf{k}|$ over a range of temperatures, along the critical isochore (see supplementary materials), for the TIP4P/2005 model (see fig. S10 for TIP4P/Ice). A sufficiently large system size was used (N = 36,424 molecules) to ensure that the linear dimension of the cubic computational cell exceeded twice the largest correlation length. The sharp increase in the structure factor at low k values is evident. Because $S(k)$ is the Fourier transform of the pair correlation function (*36*), the low-k behavior shown in Fig. 3A corresponds to an increase in long-range density fluctuations, a distinctive signature of criticality. The regressed values of the correlation length and the critical component of the isothermal compressibility are shown in Fig. 3B, plotted according to Eqs. 4 and 5. The slope of each line has been fixed at its expected 3D Ising universality class value. It can be seen that the Ising slopes provide a very good representation of the data, further confirming that the critical behavior we have identified is consistent with the 3D Ising universality class. We report an approximately threefold increase in the correlation length and a corresponding approximately fivefold increase in the compressibility. An even closer approach to criticality for this large size (from the present $T/T_c - 1 \approx 0.04$ to, say, 0.001) is beyond current computational capabilities. Undertaking such an investigation, when it becomes possible, would provide a computational probing of criticality comparable in proximity to experimental studies of ordinary vapor-liquid criticality (*37*).

Our calculations, probing the boundaries of what is computationally possible in this area at present, provide clear evidence of the presence of a metastable critical point in the deeply supercooled region of the TIP4P/2005 and TIP4P/Ice models of water as well as consistency with the Ising universality class. TIP4P/2005 and TIP4P/Ice are among the most accurate classical models of water, having in particular been demonstrated to describe water's complex crystalline phase diagram with semiquantitative accuracy (*30*, *31*). Previously, rigorous free energy methods have been used to demonstrate the presence of a LLPT in the less accurate ST2 model (*20*, *25*–*28*), subsequently confirmed by anomalous scattering calculations (*33*).

The TIP4P/2005 and TIP4P/Ice models, although among the most realistic classical models of water, are not accurate enough to endow the present calculations with predictive value for the location of the critical point in water. The critical parameters of the two models differ by ~10% in temperature (but substantially less in pressure and density). The significance of this study is the demonstration that a LLCP is not a fortuitous effect in the less accurate ST2 model but is likely a considerably more general feature that can be observed, albeit with substantial numerical effort, in quite accurate classical models. The precise determination of the location of the critical point in these models opens the possibility of tackling several open questions connected with the existence of a LLCP. Specifically, we refer to the interplay between critical fluctuations and nucleation (*38*, *39*), the nucleation of a low-density liquid from within a high-density liquid and vice versa, and the possibility of highlighting specific features associated with the LLPT that may help design experiments capable of discriminating between different thermodynamic scenarios. It is also important to test whether our findings are confirmed when using even more accurate (but computationally far more expensive) potentials (*40*) and including nuclear quantum effects (*41*).

REFERENCES AND NOTES

1. F. Franks, *Water: A Matrix for Life* (RSC Paperbacks, Royal Society of Chemistry, ed. 2, 2000).
2. P. Ball, *Proc. Natl. Acad. Sci. U.S.A.* **114**, 13327–13335 (2017).
3. C. G. Salzmann, *J. Chem. Phys.* **150**, 060901 (2019).
4. F. H. Stillinger, *Science* **209**, 451–457 (1980).
5. J. Russo, K. Akahane, H. Tanaka, *Proc. Natl. Acad. Sci. U.S.A.* **115**, E3333–E3341 (2018).
6. H. E. Stanley, J. Teixeira, *J. Chem. Phys.* **73**, 3404–3422 (1980).
7. P. G. Debenedetti, *J. Phys. Condens. Matter* **15**, R1669–R1726 (2003).
8. R. J. Speedy, C. A. Angell, *J. Chem. Phys.* **65**, 851–858 (1976).
9. S. Sastry, P. G. Debenedetti, F. Sciortino, H. E. Stanley, *Phys. Rev. E* **53**, 6144–6154 (1996).
10. P. H. Handle, T. Loerting, F. Sciortino, *Proc. Natl. Acad. Sci. U.S.A.* **114**, 13336–13344 (2017).
11. N. J. Hestand, J. L. Skinner, *J. Chem. Phys.* **149**, 140901 (2018).
12. J. A. Sellberg *et al.*, *Nature* **510**, 381–384 (2014).

13. K. H. Kim *et al.*, *Science* **358**, 1589–1593 (2017).
14. G. Pallares *et al.*, *Proc. Natl. Acad. Sci. U.S.A.* **111**, 7936–7941 (2014).
15. K. Amann-Winkel *et al.*, *Proc. Natl. Acad. Sci. U.S.A.* **110**, 17720–17725 (2013).
16. P. H. Poole, F. Sciortino, U. Essmann, H. E. Stanley, *Nature* **360**, 324–328 (1992).
17. A. K. Soper, *J. Chem. Phys.* **150**, 234503 (2019).
18. O. Mishima, H. E. Stanley, *Nature* **392**, 164–168 (1998).
19. S. Woutersen, B. Ensing, M. Hilbers, Z. Zhao, C. A. Angell, *Science* **359**, 1127–1131 (2018).
20. J. C. Palmer, P. H. Poole, F. Sciortino, P. G. Debenedetti, *Chem. Rev.* **118**, 9129–9151 (2018).
21. J. C. Palmer, R. S. Singh, R. Chen, F. Martelli, P. G. Debenedetti, *Mol. Phys.* **114**, 2580–2585 (2016).
22. E. B. Moore, V. Molinero, *Nature* **479**, 506–508 (2011).
23. Y. Li, J. Li, F. Wang, *Proc. Natl. Acad. Sci. U.S.A.* **110**, 12209–12212 (2013).
24. Y. Ni, J. L. Skinner, *J. Chem. Phys.* **144**, 214501 (2016).
25. J. C. Palmer *et al.*, *Nature* **510**, 385–388 (2014).
26. F. Sciortino, I. Saika-Voivod, P. H. Poole, *Phys. Chem. Chem. Phys.* **13**, 19759–19764 (2011).
27. T. A. Kesselring, G. Franzese, S. V. Buldyrev, H. J. Herrmann, H. E. Stanley, *Sci. Rep.* **2**, 474 (2012).
28. Y. Liu, J. C. Palmer, A. Z. Panagiotopoulos, P. G. Debenedetti, *J. Chem. Phys.* **137**, 214505 (2012).
29. A. M. Ferrenberg, R. H. Swendsen, *Phys. Rev. Lett.* **63**, 1195–1198 (1989).
30. J. L. F. Abascal, C. Vega, *J. Chem. Phys.* **123**, 234505 (2005).
31. J. L. F. Abascal, E. Sanz, R. García Fernández, C. Vega, *J. Chem. Phys.* **122**, 234511 (2005).
32. N. B. Wilding, A. D. Bruce, *J. Phys. Condens. Matter* **4**, 3087–3108 (1992).
33. J. Guo, R. S. Singh, J. C. Palmer, *Mol. Phys.* **116**, 1953–1964 (2018).
34. L. S. Ornstein, F. Zernike, *Proc. Sect. Sci. K Ned. Akad. Wet.* **17**, 793 (1914).
35. M. E. Fisher, *J. Math. Phys.* **5**, 944–962 (1964).
36. H. E. Stanley, *Introduction to Phase Transitions and Critical Phenomena* (Oxford Univ. Press, 1971).
37. J. V. Sengers, J. M. H. L. Sengers, *Annu. Rev. Phys. Chem.* **37**, 189–222 (1986).
38. K. Binder, *Proc. Natl. Acad. Sci. U.S.A.* **111**, 9374–9375 (2014).
39. R. Kurita, H. Tanaka, *Proc. Natl. Acad. Sci. U.S.A.* **116**, 24949–24955 (2019).
40. G. A. Cisneros *et al.*, *Chem. Rev.* **116**, 7501–7528 (2016).
41. B. Cheng, E. A. Engel, J. Behler, C. Dellago, M. Ceriotti, *Proc. Natl. Acad. Sci. U.S.A.* **116**, 1110–1115 (2019).
42. P. G. Debenedetti, F. Sciortino, G. H. Zerze, Data for "Second critical point in two realistic models of water," Version 1, Zenodo (2020); https://doi.org/10.5281/zenodo.3836542.

ACKNOWLEDGMENTS

The simulations presented in this work were performed on computational resources managed and supported by Princeton Research Computing, a consortium of groups including the Princeton Institute for Computational Science and Engineering (PICSciE) and the Office of Information Technology's High Performance Computing Center and Visualization Laboratory at Princeton University, and on computational resources managed and supported by the Physics Department of Sapienza University Rome. **Funding:** P.G.D. acknowledges support from the National Science Foundation (grant CHE-1856704). F.S. acknowledges support from MIUR-PRIN 2018 (grant 2017Z55KCW). **Author contributions:** P.G.D. and F.S. conceived of the project. P.G.D., F.S., and G.H.Z. designed the calculations, and F.S. and G.H.Z. performed the calculations. All authors analyzed the data. P.G.D. wrote the paper, and all authors edited the paper. **Competing interests:** None declared. **Data and materials availability:** GROMACS codes used to perform the simulations in this work are publicly available (http://manual.gromacs.org/documentation/). The input files for simulations and energy, density, and structure factor data underlying the conclusions of this work are archived in Zenodo (*42*). All other data needed to evaluate the conclusions in this paper are present either in the main text or the supplementary materials.

SUPPLEMENTARY MATERIALS

science.sciencemag.org/content/369/6501/289/suppl/DC1
Materials and Methods
Supplementary Text
Figs. S1 to S10
Tables S1 to S4
References (*43*–*58*)

30 March 2020; accepted 27 May 2020
10.1126/science.abb9796

Second critical point in two realistic models of water

Pablo G. Debenedetti, Francesco Sciortino and Gül H. Zerze

Science **369** (6501), 289-292.
DOI: 10.1126/science.abb9796

Liquid-liquid critical point of water

Despite a broad range of experimental observations that indirectly point out the possible existence of a liquid-liquid phase transition in deeply supercooled water, no unambiguous experiment has shown this yet. The challenges of performing experiments under such conditions are associated with the inevitable rapid crystallization of the metastable liquid state, and therefore computational simulations become a crucial alternative. Using two accurate classical models of water and long (more than 40 microseconds) isobaricisothermal molecular dynamics simulations, Debenedetti *et al.* provide strong computational evidence of the presence of a second metastable liquid-liquid critical point in the deeply supercooled region that has critical behavior consistent with the three-dimensional Ising universality class.

Science this issue p. 289